Weed Science 2015 63:377–387

Comparative Phytotoxicity Assays of the Herbicide Alloxydim and Its Main Identified Photoproduct in Cereal and Broadleaves Crops

Pilar Sandín-España, Beatriz Sevilla-Morán, Mercedes Villarroya-Ferruz, José L. Alonso-Prados, and M. Inés Santín-Montanyá*

When herbicides are sprayed in the field, a proportion of the herbicide falls onto leaves and soil surfaces, where it can be exposed to sunlight, generating photoproducts that can be more toxic and/or persistent than the parent substance and affect human health and the environment. The aim of this study was to identify the photoproducts of the herbicide alloxydim in leaf and soil model systems and to perform phytotoxicity studies. Alloxydim was rapidly photodegraded in systems simulating plant cuticles and soil surfaces, with half-lives ranging from 1 to 30 min. The main by-product, identified by LC-Qtof-MS as deallyoxylated alloxydim, was more stable than the active substance. The EC_{50} values on root lengths of different varieties of wheat plants and one grass weed ranged from 0.38 to 0.50 mg L^{-1} for alloxydim. In contrast, the EC_{50} values for deallyoxylated alloxydim ranged from 94 to 600 mg L^{-1} in the same species and in crops where the herbicide was applied. Special attention should be given to alloxydim degradation products because of the rapid degradation of this herbicide. Comparative bioassay studies between alloxydim and its photostable by-product showed that the by-product presents low phytotoxicity, whereas alloxydim can cause injury to neighboring and succeeding cereal crops.

Nomenclature: Alloxydim.

Key words: Herbicides, degradation products, phytotoxicity, bioassay.

After herbicides are sprayed in the field, the highest initial herbicide concentrations are generally present on the plant leaves, soil, and water to which direct application was made. However, relatively few pesticide applications are made directly and exclusively to the target pest, and most treatment methods rely on the application of enough pesticide that exposure to the pest species reaches efficacious levels. It is known that a major proportion of the herbicide sprayed in the field falls down to the soil surface (Sandín-España and Sevilla-Morán 2012). Once on plant leaves and soil surfaces, the herbicide is directly exposed to sunlight. Because of the specific environments of these matrices, herbicides can be photodegraded in a quite different manner than occurs in an aqueous environment, yielding different degradation products or different degradation rates.

Because the plant cuticle represents a complex mixture of many compounds that may act as photosensitizers, quenchers, and potential reaction partners (Monadjemi et al. 2012), model photoreactions in organic solvents simulating the natural constituents of cutin and plant waxes are often evaluated. These simple models, introduced by Schwack (Schippers and Schwack 2008; Schynowski and Schwack 1996), have proved to be the best practical way to study possible reaction pathways and product formation prior to studies in more complex natural environments. Furthermore, the resulting products can effectively be used as analytical standards for further studies in natural environments.

It is well known that the study of herbicide transformation products (TPs) is of paramount importance because some of these TPs present similar toxicity as the parent compound, and in some cases, these transformation products can be even more toxic and persistent than the active substance (Boxall et al. 2004; Mahmoud et al. 2014; Scrano et al. 2002; Smith et al. 2005; Stoklosa et al. 2012). Thus, information about degradation products, such as their identity, persistence in the environment, and toxicity, is necessary to understand the environmental fate of the active substance and evaluate its risk. Furthermore, the current legislation in developed countries aims to prevent harmful effects on human and animal health and on the environment (Villaverde et al. 2014). Thus, information about degradation products, such as their identity, persistence in the environment and toxicity, is necessary to understand the environmental fate of the active substance and evaluate its risk.

DOI: 10.1614/WS-D-14-00122.1

* First through fourth authors: Researchers, DTEVPF—Unit of Plant Protection Products, INIA, Madrid, 28040; fifth author: Researcher, Department of Plant Protection, INIA, Madrid, 28040. Corresponding author's E-mail: sandin@inia.es

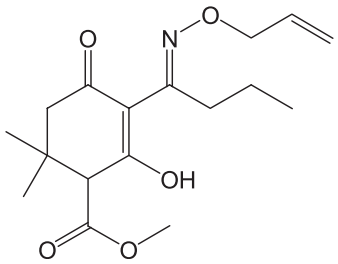

Figure 1. Chemical structure of alloxydim.

It is known that cyclohexanedione herbicides are photochemically unstable and are easily degraded by sunlight irradiation (Sandín-España and Sevilla-Morán 2012; Sandín-España et al. 2012). Thus, solar radiation could be the main abiotic transformation process affecting the efficiency of these herbicides. Furthermore, several authors have suggested the possibility that some transformation products induce phytotoxicity in grasses (Campbell and Penner 1985; Shoaf and Carlson 1992).

Alloxydim (Figure 1) is a selective postemergence herbicide belonging to the cyclohexanedione class that is used to control gramineous weeds in soybean [*Glycine max* (L.) Merr.], sugarbeet (*Beta vulgaris* L.), and other broadleaf crops. Alloxydim absorbs light at wavelengths above 290 nm, so photochemical reactions caused by sunlight irradiation can be presumed. Little is known about its degradation on plant and soil surfaces (Hashimoto et al. 1979a, 1979b; Ono et al. 1984; Soeda et al. 1979; Veerasekaran and Catchpole 1982), and the majority of the photolysis studies of this compound have been performed in aqueous media (Iwataki and Hirono 1979; Sandín-España et al. 2013a; Sevilla-Morán et al. 2008). In previous studies performed by our group, we observed rapid degradation in river water with a half-life of 3.4 h under natural sunlight, and we identified a deallyoxylated compound and the *Z* isomer of alloxydim as the main by-products (Sandín-España et al. 2013a).

The objective of the present study was to determine the photodegradation and reaction pathways of alloxydim in various environments with the use of several model solvents simulating leaf and soil surfaces. To study the photoreactivity and possible photodegradation pathways of alloxydim on plant surfaces, model experiments in the presence of cyclohexane, cyclohexene, isopropanol, and ethanol were performed. To study the behavior of alloxydim in soil systems, its photolysis was simulated on glass plates as thin films and on silica gel plates to simulate the adsorbed phase of the herbicide. Furthermore, the resulting by-product was successfully isolated and used as an analytical standard to perform studies on its phytotoxicity.

Among the different methods used to investigate responses to herbicides, soil-free assays (e.g., assays in Petri dishes or pots and in vitro tests) are the most attractive for the early detection of herbicide phytotoxicity. These techniques offer several advantages, as they are rapid and simple and can detect very low phytotoxic levels of residues and their bioavailability (Sandín-España et al. 2013b; Santín-Montanya et al. 2007). Kapanen and Itavaara (2001) proposed seed germination and seedling growth as reliable indicators of growth response to different chemicals, though there is still a lack of data concerning the toxicity of their photoproducts on the germination process of plants.

Consequently, the following objective of this work was to compare the responses of different plant species to alloxydim and its main photoproduct and to assess whether seed germination bioassays can be successfully used as a method to measure phytotoxicity in successive crops and nontarget plants.

Materials and Methods

Reagents and Solutions. Alloxydim was acquired from Dr. Ehrenstorfer GmbH (Augsburg, Germany) as the sodium salt (98% purity) and was used without further purification.

Ultrapure water was obtained with the use of a Millipore system (Milli-Q-50 18 mΩ), and formic acid (p.a.) was obtained from Merck (Darmstadt, Germany). Commercial mineral water (FontVella) was purchased from a local supermarket. Acetonitrile (HPLC far UV grade), methanol (HPLC grade), 2-propanol (HPLC grade), cyclohexane (HPLC grade), and ethyl acetate (HPLC grade) were supplied by Labscan (Stillorgan, Co., Dublin, Ireland). Ethanol (99.9% pure) and cyclohexene (99% pure) were purchased from Panreac Química SAU (Barcelona, Spain) and Acrōs Organics BVBA (Geel, Belgium), respectively.

Stock solutions of alloxydim (100 mg L^{-1}) in ethanol and 2-propanol were prepared by directly dissolving the appropriate amount of the herbicide in the respective solvent. Because alloxydim shows low solubility in cyclohexane and cyclohexene, these stock solutions were prepared at lower concentrations (10 mg L^{-1}) by first dissolving the herbicide in the minimum amount of ethyl acetate (3 ml). All stock solutions of alloxydim were stored at 4 C in the dark and were used to prepare more dilute

https://doi.org/10.1614/WS-D-14-00122.1 Published online by Cambridge University Press

standard solutions (5 mg L^{-1}) through the addition of the respective solvent.

Irradiation Experiments. Simulated sunlight for the photodegradation experiments was provided by a Suntest CPS+ apparatus from Atlas (Linsengericht, Germany) equipped with a xenon arc lamp (1,500 W) and a special glass filter restricting the transmission at wavelengths below 290 nm. All photochemical studies were performed at an irradiation intensity of 750 W m^{-2}. A Suncool chiller was used to maintain a mean internal temperature of 25 ± 1 C. This setup was an appropriate source of simulated sunlight because it provided a wavelength distribution close to that of natural sunlight and a constant irradiance.

Three replicates were carried out for each photodegradation experiment, and experiments were carried out until complete herbicide disappearance. Concurrently with the irradiation experiments, control experiments in the absence of radiation were performed under identical conditions to evaluate whether processes other than photodegradation occurred.

Nonaqueous solutions of alloxydim in ethanol, 2-propanol, cyclohexane, and cyclohexene were exposed to simulated solar radiation in round capped quartz cuvettes with magnetic stirring. At selected time intervals, aliquots were withdrawn and subsequently analyzed by HPLC-DAD to follow the reaction kinetics. Before chromatographic analysis, the solvent of the samples in cyclohexane and cyclohexene was removed with the use of a vacuum centrifuge (Eppendorf AG, Hamburg, Germany) for 10 min, and the residue was dissolved in methanol, whereas the samples in ethanol and 2-propanol were injected directly.

For the photolysis studies of alloxydim on a thin film, a methanolic solution of the herbicide (50 µL, 100 mg L^{-1}) was placed on glass plates (6 cm ID). The methanol was evaporated at room temperature, leaving behind a thin layer of alloxydim. These plates were exposed to simulated solar light for different time intervals. After irradiation, the glass plates were rinsed with methanol (2 × 0.5 ml), and the extracts were analyzed with the use of HPLC-DAD to follow the reaction kinetics.

The photolysis of alloxydim in the adsorbed phase was carried out with the use of HPTLC plates (0.20 mm Silica gel C18-100) (without fluorescence indicator) purchased from Macherey-Nagel GmbH &Co. KG (Düren, Germany). Methanolic solutions of the herbicide (50 µl, 100 mg L^{-1}) were placed on silica gel plates, and the solvent was evaporated at room temperature. Spiked silica gel plates were exposed to simulated solar light for different time intervals. After irradiation, the silica gel was scraped from the plates, and the analytes were extracted with 1 ml of methanol. The extracts were then centrifuged for 3 min, and the supernatant was filtered through 0.2-µm nylon filters and injected into the chromatographic system.

Chromatographic Analysis. The photodegradation kinetics were investigated with an HPLC system (series 1100; Agilent Technologies, Palo Alto, CA) coupled to a photodiode array detector (DAD). The analytical column used was a Waters Nova-Pak® C18 column (4 µm particle size, 3.9 mm by 150 mm) with an ODS precolumn and was maintained at 25 C. The mobile phase was a mixture of water acidified with 0.1% formic acid (A) and acetonitrile (B).

A gradient method was used to follow the decay of alloxydim as well as to study the photoproduct formation during the irradiation experiments. The percentages of B in the mobile phase were as follows: 0 to 1.2 min, 50%; 1.2 to 2 min, 50 to 60%; 2 to 3 min, 60 to 70%. The separation finished at 8 min. The flow rate was 1 ml min^{-1}, and the injection volume was 20 µl.

To identify the photoproducts, mass spectrometry experiments were performed with the use of an HPLC coupled to a hybrid Qtof mass spectrometer. The analytical method has been described in a previous work from our group (Sevilla-Morán et al. 2008).

Isolation of the Main Degradation Product. For the bioassay experiments, the main photoproduct, deallyoxylated alloxydim, was obtained from concentrated aqueous solutions of alloxydim (500 mg L^{-1}). After irradiating this solution until the complete disappearance of alloxydim (110 h), solid phase extraction (SPE) was used to extract and isolate the main photoproduct. The irradiated sample was passed through Isolute ENV+ cartridges (500 mg, 3 ml) (Symta, Madrid, Spain) and extraction was performed under gravity with an elution volume of 3 × 2 ml of methanol. The eluate was evaporated to dryness under a gentle air stream and stored at 4 C in the dark.

Seed Germination Bioassays. The study was conducted with two winter wheats, rivet wheat [*Triticum turgidum* L. var. *durum* (cv. Nita)] and

https://doi.org/10.1614/WS-D-14-00122.1 Published online by Cambridge University Press

[*Triticum aestivum* L. (cv. Pavon)], one grass weed ripgut brome (*Bromus diandrus* L.), and two dicotyledonous crops: sugar beet and tomato (*Solanum lycopersicum* L. cv. Marmande). The analytical standard alloxydim–sodium and the photoproduct deallyoxylated alloxydim were used as the active ingredients.

Seed germination bioassays were conducted in a growth chamber with 16 h of light (illumination 100 μE m^{-2} s^{-1}) at 22 ± 1 C and 8 h of darkness at 16 ± 1 C. Twenty seeds of all species assayed were distributed in a petri dish (9-cm diameter) on double-layered Whatman No. 1 filter paper. The seeds were then treated with 15 ml of either alloxydim at six different herbicide concentrations ranging from 0 to 5 mg L^{-1} or with deallyoxylated alloxydim at concentrations of 0 to 800 mg L^{-1}. The experimental work followed a completely randomized design with three replicates, and each herbicide dose was replicated three times. Appropriate control systems containing no herbicide (with ultrapure water) were included in each experiment, and the seeds were regularly checked for moisture. The control and treated seeds were grown under the same conditions of temperature and photoperiod.

The effects of alloxydim and deallyoxylated alloxydim were measured by the main germination parameters of the seeds (root length and coleoptile length) recorded 5 d after seeding (DAS) for wheat and 9 DAS for ripgut brome, sugarbeet, and tomato. In each experiment, the seed sensitivity of each species was determined with the use of the dose–response curves of the root and coleoptile length. The EC_{50} values (herbicide doses required to cause a 50% inhibition of root/coleoptile growth) were calculated with the use of nonlinear regression analysis of the herbicide doses vs. percent inhibition data.

Data Analysis. The photolysis rates of alloxydim were described by first-order kinetics given by the following equation:

$$C_t = C_0 e^{-kt}, \quad [1]$$

where C_0 is the initial concentration of alloxydim, C_t is the concentration at irradiation time t, and k is the rate constant of the photodegradation process.

The half-lives ($t_{1/2}$) of the photolysis processes were also determined. This parameter is defined as the time taken for the alloxydim concentration to fall to half of its initial value and is related to the rate constant, k, by means of the equation $t_{1/2} = \ln 2/k$.

The quantum yield for clethodim was calculated in different solvents according to the method described by Swanson et al. (1995).

The kinetic parameters for the photodegradation of alloxydim were calculated as the means of three replicates. Moreover, one-way analyses of variance (ANOVA) were conducted to determine differences between the rate constants of alloxydim under the different experimental conditions studied at the 0.05 significance level.

In the bioassay experiments, nonlinear regression was used to fit the log-logistic equation (Seefeldt et al. 1995) to the root length and coleoptile length data versus dose in each species. The equation of these curves is

$$Y = C + ((D - C)/\{1 + \exp[b \cdot \ln(X) - \ln(EC_{50} + 1)]\}), \quad [2]$$

where Y is the root length or coleoptile length (cm), X is the herbicide dose (mg L^{-1}), D is the upper asymptote (maximum root growth of plants), C is the lower asymptote (minimum root growth of plants), b is the slope of the curve around the EC_{50}, and EC_{50} is the dose giving 50% root/coleoptile length inhibition.

All analyses were performed with the use of Statgraphics Plus v.5.0 software (Copyright© 1994–2000 Statistical Graphics Corp. STATPOINT Technologies, Inc.).

Results and Discussion

Kinetics Analysis. It is known that photolysis is an efficient route for the degradation of alloxydim in different aqueous media because the herbicide absorbs above 290 nm (e.g., $\varepsilon_{290\ nm} = 18{,}011\ L\ mol^{-1}\ cm^{-1}$) (Sandín-España et al. 2013a; Sevilla-Morán et al. 2008).

Similar to that in aqueous media, the UV absorption spectra of alloxydim in the organic solvents showed strong absorption above 290 nm (e.g., $\varepsilon_{290\ nm(ethanol)} = 16{,}688\ L\ mol^{-1}\ cm^{-1}$). Moreover, the quantum yields calculated for the herbicide in these solvents were comparable to that obtained in ultrapure water ($\Phi_{clethodim\ (in\ solvents)} \approx 0.42$ vs. $\Phi\ \Phi_{clethodim\ (in\ ultrapure\ water)} = 0.26$). Therefore, it can be expected that the direct photodegradation of alloxydim occurs under the experimental conditions studied because the absorbance spectra of alloxydim in the organic solvents and the UV emission spectrum of the radiation source overlap in the region of 290 to 325 nm.

https://doi.org/10.1614/WS-D-14-00122.1 Published online by Cambridge University Press

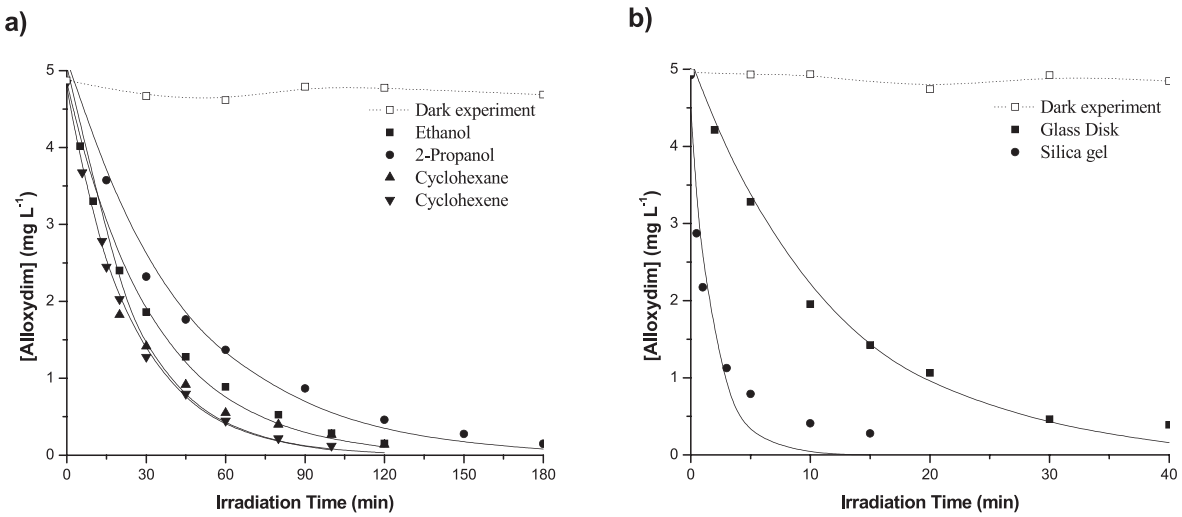

Figure 2. Photodegradation of alloxydim in different nonaqueous solutions (a) and on solid surfaces (b) under simulated solar radiation. Plots were fitted to Equation 1 ($C_t = C_0\ e^{-kt}$).

The photolysis of alloxydim was studied in different nonaqueous media to simulate the several functional groups present in plant cuticle constituents. Thus, ethanol and 2-propanol were selected as the simplest model solvents for the primary and secondary alcohol groups present in cutin acids, free fatty alcohols or sterols, whereas cyclohexane and cyclohexene were used as models of the saturated and unsaturated hydrocarbon chains of alkanes, alkenes, terpenes, lipids, and sterols. Furthermore, the photochemical behavior of alloxydim was also investigated on glass disks and on silica gel plates as surrogates for soil surfaces.

Figures 2a and 2b show the photolysis kinetics of alloxydim under simulated sunlight in organic solvents and on solid surfaces, respectively. Alloxydim rapidly photodegraded under the irradiation conditions studied, whereas no significant loss of the herbicide was observed in the dark experiments during the irradiation times of the studies performed (40 and 180 min) (Figure 2). Hence, other reactions that are not photoinitiated (thermal degradation, hydrolysis, etc.) can be discarded.

Table 1 compiles the kinetic parameters of alloxydim–sodium photolysis in nonaqueous solutions and on solid surfaces under simulated solar irradiation. The experimental data show that alloxydim was completely degraded in nonaqueous media after short irradiation times ranging from 1.7 h for cyclohexene to 3 h for 2-propanol, with calculated half-lives of 16.5 min (cyclohexane) and ½ (2-propanol). Analysis of variance showed significant differences among the rate constants of alloxydim in the solvents tested, except for in cyclohexane and cyclohexene, where the rate constants were similar (approximately $43.3 \times 10^{-3} \cdot \text{min}^{-1}$). Moreover, the phototransformation of alloxydim was faster in nonaqueous media than in aqueous media. In a previous work, the photolysis rate constant of alloxydim in mineral water was measured to be $13.65 \times 10^{-3}\ \text{min}^{-1}$ (Sandín-España et al. 2013a), whereas in this study, the rate constant in 2-propanol was $23.5 \times 10^{-3}\ \text{min}^{-1}$. This indicates that the photolysis rate of alloxydim is dependent on the composition of the reaction medium. Therefore, it can be expected

Table 1. Kinetic parameters of alloxydim–sodium photolysis in nonaqueous solutions and on solid surfaces under simulated solar irradiation (750 W m^{-2}). The different letters show significant differences according to least significant difference tests (LSDs) at a significance level of 95%.

	k	$t_{1/2}$	R^2
	$10^{-3} \cdot \text{min}^{-1}$	min	
Ethanol	30.7 ± 3.37 a	22.6 ± 0.4	0.99
2-propanol	23.5 ± 2.9 b	29.6 ± 0.5	0.99
Cyclohexane	44.6 ± 6.7 c	15.6 ± 0.5	0.98
Cyclohexene	41.9 ± 3.9 c	16.5 ± 0.3	0.99
Glass disk	85.3 ± 13.3 d	8.1 ± 0.4	0.98
Silica gel	591.2 ± 0.3 e	1.2 ± 0.4	0.92

https://doi.org/10.1614/WS-D-14-00122.1 Published online by Cambridge University Press

that alloxydim will suffer rapid photolysis on plant surfaces and that the rate of this degradation process will depend on the functional groups present in the plant cuticle.

Regarding its photolysis on solid surfaces, alloxydim was completely degraded after 40 min on the glass plates and after 15 min on the silica gel plates. Surprisingly, although the layers of silica could attenuate the light irradiation, a higher alloxydim degradation rate was observed on the silica gel plates compared to on the glass plates. Thus, the half-life of alloxydim on the silica gel plates was 1.2 ± 0.4 min, and that on the glass plates was 8.1 ± 0.4 min. This result could be attributed to the interaction between the molecules of alloxydim with the functional groups of the silica gel, favoring the photodegradation of the herbicide, whereas the glass surface is an inert material.

With regard to the photodegradation on solid versus liquid media, the rate of alloxydim photolysis was faster on solid surfaces than in aqueous solutions or in nonaqueous media. This increase in the photodegradation rate on solid surfaces could be attributed to the absence of solvent. It is known that solvents can attenuate the radiation by scattering or can deactivate excited molecules of the herbicide by physical quenching as consequence of the solvent cage effect (Wayne and Wayne 1996). Besides, in the solid-surface experiments, the radiation is not attenuated by transmission through the quartz or the caps of the cuvettes and directly reaches the herbicide.

Identification of Degradation Products. During the irradiation of alloxydim, two different photoproducts (DP1 and DP2) were detected by HPLC-DAD. Both photoproducts presented retention times shorter than that of alloxydim, showing a more polar character than the parent herbicide, which made them highly mobile. Thus, these photoproducts may be potential contaminants of aqueous media and soil.

Because of the lack of commercial standards, the photoproducts DP1 and DP2 were separated and identified by means of HPLC-ESI-Qtof-MS. By means of the Qtof analyzer, it was possible to isolate the $[M+H]^+$ ions of both photoproducts for their subsequent fragmentation and thus to study their MS/MS fragmentation pattern. The MS/MS spectra of photoproducts DP1 and DP2 are presented in Figure 3, together with the proposed fragmentation mechanism for their main fragments.

Photoproduct DP2 exhibited an $[M+H]^+$ ion at the same nominal mass as alloxydim (m/z = 324). Moreover, the MS/MS analysis of the molecular ion (m/z = 324.1810) gave a spectrum that closely resembled the protonated molecule of alloxydim (Figure 3a). Thus, the main fragments of DP2 were formed as consequence of the loss of methanol and/or of 2-propenol molecules (292.1563, 266.1439, and 234.1158). On the basis of its MS/MS fragmentation and the accurate mass measurements, the DP2 photoproduct was identified as the *Z* isomer of alloxydim at the oxime ether double bond. Several authors have stated that some *E*-isomers of cyclohexanedione oxime herbicides may equilibrate with the *Z*-isomer in polar solvents (Falb et al. 1990; Sevilla-Morán et al. 2010) or in chlorinated water (Sandín-España et al. 2003). The mass spectra of photoproduct DP1 showed an even nominal mass for the protonated molecule equal to m/z 268 (Figure 3b), which indicates that it retained the nitrogen atom in its structure. The Analyst Software provided the formula of $C_{14}H_{22}O_4N$ as the most probable composition for DP1. The proposed fragmentation mechanism for the $[M+H]^+$ ion of photoproduct DP1 is illustrated in Figure 3b. The selective fragmentation of the molecular ion $[M+H]^+$ (m/z 268) led to the formation of three abundant ions at nominal masses of m/z 236.1319, 208.1354 and 180.1390. This by-product was also detected in the photodegradation of alloxydim in environmental waters (Sandín-España et al. 2013a; Sevilla-Morán et al. 2008). Although several authors have reported the formation of the corresponding enamine of alloxydim (the tautomer of deallyoxylated alloxydim), as a result of biotic or abiotic reactions in sugar beet (Soeda et al. 1979), soybean (Hashimoto et al. 1979a, 1979b), and sterilized soil (Ono et al. 1984), to the best of our knowledge, the deallyoxylated alloxydim derivative has not been previously observed in any photodegradation study on plant leaves or soil surfaces.

The kinetic evolution of both photoproducts, deallyoxylated alloxydim (DP1) and the alloxydim *Z* isomer (DP2), during photolysis was followed by means of HPLC-DAD. Their profiles were observed to be similar in the organic solvents and on the solid surfaces. Thus, in all cases, deallyoxylated alloxydim (DP1) was detected as the major product, and it reached its maximum level at the end of the irradiation time. This photoproduct appeared to be photochemically stable, allowing it to remain on soil and plant surfaces for a longer time than the active substance. In the case of plant leaves, the photoproduct DP1 can be generated and then be

https://doi.org/10.1614/WS-D-14-00122.1 Published online by Cambridge University Press

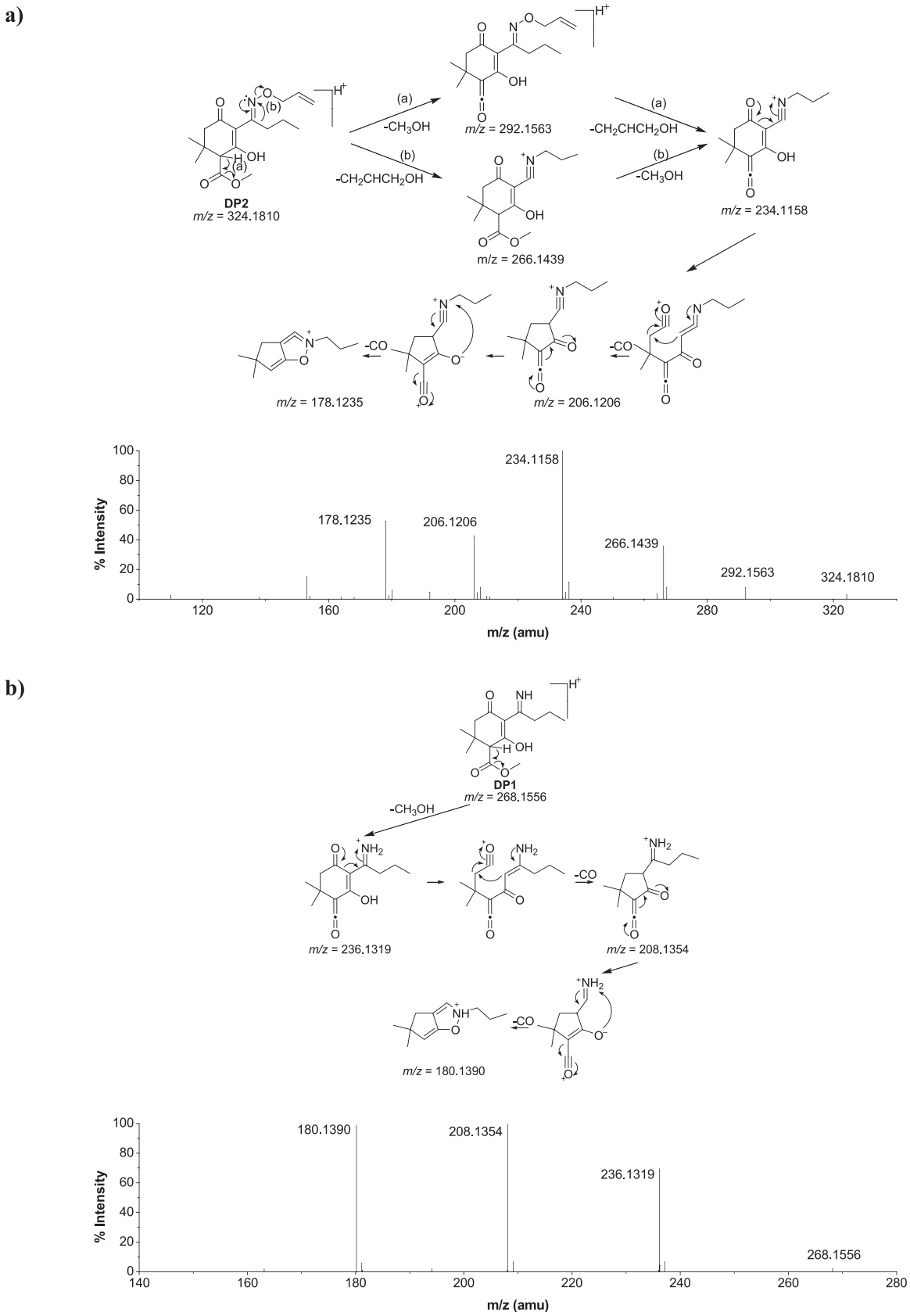

Figure 3. Chemical structures, proposed fragmentation patterns and MS/MS spectra of the photoproducts DP2 (a) and DP1 (b).

https://doi.org/10.1614/WS-D-14-00122.1 Published online by Cambridge University Press

Table 2. Parameters of the regression equations (by Seefeldt equation) that describe the relationships between increasing alloxydim and deallyoxylated alloxydim concentrations and the coleoptile length reduction of the species. The plant response to increasing doses of alloxydim and deallyoxylated alloxydim obtained in each seed germination bioassay; doses (mg L^{-1}) for 50% inhibition of the coleoptile length (EC_{50} values).

Species	Active ingredient	Upper asymptote (C)	Lower asymptote (D)	Slope (b)	EC_{50}	R^2
		cm		cm L mg^{-1} m^{-1}	mg L^{-1}	%
Triticum turgidum	Alloxydim-B 1	−12.718	5.393	1.789	10.92	96.03
L. var. *durum* cv. Nita	Alloxydim-B 2	−9.044	4.842	2.058	9.83	93.24
	Alloxydim-B 3	−16.090	5.092	2.476	10.38	97.79
	DP1-B 1	1.777	5.357	1.392	325.30	96.29
	DP1-B 2	2.352	4.987	2.631	379.99	96.23
	DP1-B 3	2.175	5.092	1.744	377.45	97.14
Triticum aestivum	Alloxydim-B 1	1.105	4.495	3.904	3.05	96.57
L. cv. Pavon	Alloxydim-B 2	0.658	4.804	2.753	4.01	96.92
	Alloxydim-B 3	1.680	4.458	6.332	3.45	93.97
	DP1-B 1	1.691	4.512	1.191	664.00	80.69
	DP1-B 2	1.215	4.889	1.029	703.94	91.59
	DP1-B 3	0.864	4.597	1.720	705.96	93.18
Bromus diandrus L.	Alloxydim-B 1	0.074	7.446	1.438	1.15	92.70
	Alloxydim-B 2	2.607	6.076	4.049	1.55	90.13
	Alloxydim-B 3	2.711	5.585	6.718	1.61	93.92
	DP1-B 1	1.376	5.556	1.670	200.04	95.09
	DP1-B 2	0.515	6.179	1.539	170.46	94.46
	DP1-B 3	0.823	6.809	1.601	244.47	96.90
Bromus vulgaris	Alloxydim-B 1	Not adjusted				
L. cv. Dulzata	Alloxydim-B 2					
	Alloxydim-B 3					
	DP1-B 1	1.713	2.504	2.4138	245.68	76.88
	DP1-B 2	1.282	2.811	1.815	237.32	96.46
	DP1-B 3	0.617	2.773	1.078	504.14	98.37
Solanum lycopersicum	Alloxydim-B 1	Not adjusted				
L. cv. Marmande	Alloxydim-B 2					
	Alloxydim-B 3					
	DP1-B 1	1.264	2.061	6.018	690.53	84.12
	DP1-B 2	1.502	2.028	8.844	604.36	81.72
	DP1-B 3	1.316	2.047	10.610	679.87	84.25

absorbed by the plant, causing unknown damages. Furthermore, because deallyoxylated alloxydim presents a higher solubility than alloxydim, there is a higher risk of contamination of ground and surface waters as a consequence of leaching and runoff processes. However, available information about this compound is still scarce. Hence, it is necessary to ascertain whether residues of this compound represent any danger to the environment.

Regarding the by-product DP2, it was formed in smaller amounts, and the maximum levels of this minor product were reached at the first stages of photolysis and then slowly decreased until its complete disappearance. Although it has been reported that the *Z* isomer (DP2) quickly reverts to the initial *E* isomer (Sandín-España et al. 2013a), it can be expected that the *Z* isomer also undergoes photolysis to form the deallyoxylated alloxydim derivative DP1.

Because of the fast photodegradation of alloxydim in the surrogate plant and soil surfaces, and because of the high amount of the deallyoxylated alloxydim photoproduct DP1 detected at the end of the experiments, it can expected that this compound is present on plant surfaces and soil matrices. This is of great importance, because different authors have suggested that the phytotoxicity of some cyclohexanedione oxime herbicides is due not only to the parent compounds, but also to their transformation products (Campbell and Penner 1985; Shoaf and Carlson 1992).

Bioassay Experiments. Clear differences were observed in the sensitivity of the tested species to the herbicide alloxydim and to the photoproduct deallyoxylated alloxydim. The herbicide alloxydim is used in dicot crops against grass species; thus, as expected, this herbicide did not cause any damage in

https://doi.org/10.1614/WS-D-14-00122.1 Published online by Cambridge University Press

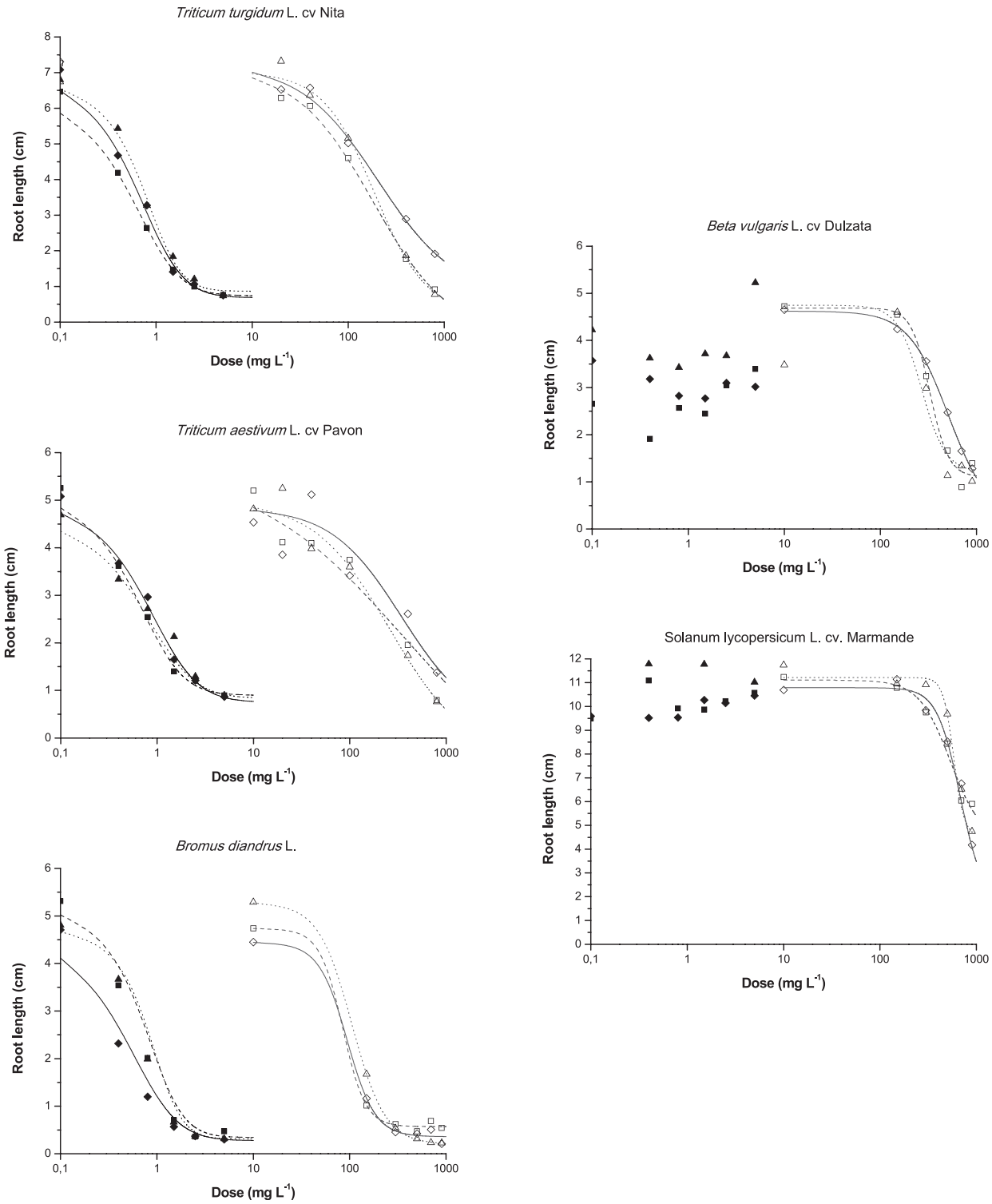

Figure 4. Dose–response curves for alloxydim and its photoproduct, deallyoxylated alloxydim (DP1), from seed germination bioassays for the root length of all species assayed. Plots were fitted to log-logistic equation 2 ($Y = C + ((D - C)/\{1 + \exp[b \cdot \ln(X) - \ln(EC_{50}+1)]\})$).

the dicotyledonous species (sugarbeet and tomato). The root and coleoptile lengths of all grass species (ripgut brome and wheat) assayed were significantly affected at a low dose. However, we observed that the photoproduct deallyoxylated alloxydim caused injury in the germination bioassays of all species tested (Table 2, Figure 4), although the doses employed were much higher than those used for alloxydim.

The EC_{50} values were obtained for both alloxydim and deallyoxylated alloxydim. The EC_{50} values calculated from the coleoptile length were

https://doi.org/10.1614/WS-D-14-00122.1 Published online by Cambridge University Press

higher than those obtained from the root length, indicating that the roots of all species were more sensitive to the herbicide and its photoproduct. These results are in accordance with previous experiments with another cyclohexanedione oxime herbicide (Sandín-España et al. 2003).

The EC_{50} values (average of three bioassays) from the root lengths of *Triticum* species and *Bromus* ranged from 0.381 to 0.503 mg L^{-1} for alloxydim. Deallyoxylated alloxydim caused root-length inhibition of all species assayed, with EC_{50} values of 94.357 mg L^{-1} in ripgut brome L., 225.718 and 314.862 mg L^{-1} in the *Triticum* species, 367.059 mg L^{-1} in sugarbeet, and 599.896 mg L^{-1} in tomato (Table 1). Regarding the coleoptile length, similar doses of deallyoxylated alloxydim produced coleoptile length inhibition in ripgut brome and sugarbeet (360.911 and 329.046 mg L^{-1}, respectively), whereas higher doses inhibited the coleoptile length of wheat and tomato (691.301 and 658.250 mg L^{-1}, respectively). Lower doses of 204.989 mg L^{-1} caused coleoptile length inhibition in ripgut brome For alloxydim, much lower doses caused coleoptile length inhibition compared to its photoproduct, with EC_{50} values of 10.377, 3.505 and 1.438 mg L^{-1} for wheat and ripgut brome, respectively (Table 2).

The results obtained in this study confirm that the different varieties of wheat plants and the grass weed (ripgut brome) employed in this study could be susceptible to cyclohexanedione herbicides during the germination process. The foregoing results suggest that alloxydim can cause damage during seed germination and to the seedlings of cereal succeeding crops, neighboring cereal crops, and on nontarget plants. Nevertheless, we observed that the doses of the photoproduct deallyoxylated alloxydim required to cause injury in seed germination and to the seedlings of all tested species were up to 200-fold higher compared to alloxydim. Therefore, taking into account the herbicide doses employed in the field, it is very unlikely to find these high concentrations in the soil, although the possibility for accumulation cannot be discounted because of the photostability of this byproduct. Further studies on the degradation pathway would be desirable.

The evaluation of an herbicide's phytotoxicity by biological testing is therefore extremely important for screening its suitability for agricultural applications. We have demonstrated that bioassays are analytical tools that can be used to assess exposure to herbicides acting by a common mode of action. The information obtained does not directly indicate ecological risk, although a strong connection between biochemical response levels and seed germination or seedling effects could be established.

In summary, the results of this work indicate that the photodegradation of alloxydim in surrogates of soil and plant surfaces is an important route for the dissipation of alloxydim herbicides, which have half-lives of less than an hour in the different modes studied. Therefore, it is extremely important to investigate the degradation products of alloxydim further. LC-Qtof-MS was employed to identify the two photoproducts formed: the *Z*-isomer of alloxydim and the major compound, identified as deallyoxylated alloxydim resulting from the cleavage of the N–O of the oxime bond. Surprisingly, this by-product is far more photostable than the active substance, and further studies are therefore desirable to assess the fate of deallyoxylated alloxydim in the environment.

The results obtained in the germination bioassays performed showed that the plant roots were more sensitive to both substances tested than coleoptile length was. However, the effect of the main photoproduct on the germination of the plant species tested at the concentration expected in the soil was negligible. Conversely, alloxydim inhibited the seed germination of cereal succeeding crops and neighboring cereal crops. Therefore, special care should be taken to achieve the sustainable use of this herbicide in the field.

Literature Cited

Boxall ABA, Sinclair CI, Fenner K, Kolpin DW, Maund SJ (2004) When synthetic chemicals degrade in the environment. Environ Sci Technol 38:368A–375A

Campbell JR, Penner D (1985) Abiotic transformations of sethoxydim. Weed Sci 33:435–439

Falb LN, Bridges DC, Smith AE (1990) Effects of pH and adjuvants on clethodim photodegradation. J Agric Food Chem 38:875–878

Hashimoto Y, Ishihara K, Soeda Y (1979a) Fate of alloxydim–sodium on or in soybean plants. J Pestic Sci 4:299–304

Hashimoto Y, Ishihara K, Soeda Y (1979b) Nature of the residue in soybean plant after treatment of alloxydim–sodium. J Pestic Sci 4:375–378

Iwataki I, Hirono Y (1979) The chemical structure and herbicidal activity of alloxydim–sodium and related compounds. Pages 235–243 *in* Geissbühler H, Brooks GT, Kearney PC, eds. Advances in Pesticide Science. Oxford, UK: Pergamon Press

Kapanen A, Itavaara M (2001) Ecotoxicity tests for compost applications. Ecotox Environ Safe 49:1–6

Mahmoud WMM, Toolaram AP, Menz J, Leder C, Schneider M, Küemmerer K (2014) Identification of phototransformation products of thalidomide and mixture toxicity assessment:

https://doi.org/10.1614/WS-D-14-00122.1 Published online by Cambridge University Press

an experimental and quantitative structural activity relationships (QSAR) approach. Water Res 49:11–22
Monadjemi S, Ter Halle A, Richard C (2012) Reactivity of cycloxydim toward singlet oxygen in solution and on wax film. Chemosphere 89:269–273
Ono S, Shiotani H, Ishihara K, Tokieda M, Soeda Y (1984) Degradation of the herbicide alloxydim–sodium in soil. J Pestic Sci 9:471–480
Sandín-España P, Llanos S, Magrans JO, Alonso-Prados JL, García-Baudín JM (2003) Optimization of hydroponic bioassay for herbicide tepraloxydim by using water free from chlorine. Weed Res 43:451–457
Sandín-España P, Sevilla-Morán B (2012) Pesticide degradation in water. Pages 79–130 *in* Rathore HS, Nollet LML, eds. Pesticides: Evaluation of Environmental Pollution. Boca Raton, FL: CRC Press
Sandín-España P, Sevilla-Morán B, Alonso-Prados JL, Santín-Montanya I (2012) Chemical behaviour and herbicidal activity of cyclohexanedione oxime herbicides. Pages 75–102 *in* Naguib M, Hasaneen AEG, eds. Herbicides—Properties, Synthesis and Control of Weeds. Rijeka, Croatia: InTech
Sandín-España P, Sevilla-Morán B, Calvo L, Mateo-Miranda M, Alonso-Prados JL (2013a) Photochemical behavior of alloxydim herbicide in environmental waters. Structural elucidation and toxicity of degradation products. Microchem J 106:212–219
Sandín-España P, Sevilla-Morán B, Villarroya-Ferruz M, Alonso-Prados JL, Santín-Montanyá I (2013b) Photolysis experiments on alloxydim herbicide and biological response of its transformation product. Pages 151–174 *in* Kobayashi D, Watanabe E, eds. Handbook on Herbicides: Biological Activity, Classification and Health & Environmental Implications. New York: Nova Science Publishers
Santín-Montanya I, Sandín-España P, García Baudín JM, Coll-Morales J (2007) Optimal growth of *Dunaliella primolecta* in axenic conditions to assay herbicides. Chemosphere 66:1315–1322
Schippers N, Schwack W (2008) Photochemistry of imidaclopprid in model systems. J Agric Food Chem 56:8023–8029
Schynowski F, Schwack W (1996) Photochemistry of parathion on plant surfaces: relationship between photodecomposition and iodine number of the plant cuticle. Chemosphere 33:2255–2562
Scrano L, Bufo SA, D'Auria M, Meallier P, Behechti A, Shramm KW (2002) Photochemistry and photoinduced toxicity of acifluorfen, a diphenyl-ether herbicide. J Environ Qual 31:268–274
Seefeldt SS, Jensen JE, Patrick Fuerst E (1995) Log-logistic analysis of herbicide dose–response relationships. Weed Technol 9:218–225
Sevilla-Morán B, Alonso-Prados JL, García-Baudín JM, Sandín-España P (2010) Indirect photodegradation of clethodim in aqueous media. By-product identification by quadrupole time-of-flight mass spectrometry. J Agric Food Chem 58:3068–3076
Sevilla-Morán B, Sandín-España P, Vicente-Arana MJ, Alonso-Prados JL, García-Baudín JM (2008) Study of alloxydim photodegradation in the presence of natural substances: elucidation of transformation products. J Photochem Photobiol A 198:162–168
Shoaf AR, Carlson WC (1992) Stability of sethoxydim and its degradation products in solution, in soil, and on surfaces. Weed Sci 40:384–389
Smith MC, Shaw DR, Miller DK (2005) In-field bioassay to investigate the persistence of imazaquin and pyrithiobac. Weed Sci 53:121–129
Soeda Y, Ishihara K, Iwataki I, Kamimura H (1979) Fate of a herbicide ^{14}C-alloxydim-sodium in sugar beets. J Pestic Sci 4:121–128
Stoklosa A, Matraszek R, Isman MB, Upadhyaya MK (2012) Phytotoxic activity of clove oil, its constituents, and its modification by light intensity in broccoli and common lambsquarters (*Chenopodium album*). Weed Sci 60:607–611
Swanson MB, Ivancic WA, Saxena AM, Allton JD, O'Brien GK, Suzuki T, Nishizawa H, Nokata M (1995) Direct photolysis of fenpyroximate in a buffered aqueous solution under a xenon lamp. J Agric Food Chem 43:513–518
Veerasekaran P, Catchpole AH (1982) Studies on the selectivity of alloxydim–sodium in plants. Pestic Sci 13:452–62
Villaverde JJ, Sevilla-Morán B, Sandín-España P, López-Goti C, Alonso-Prados JL (2014) Biopesticides in the framework of the European Pesticide Regulation (EC) No. 1107/2009. Pest Manag Sci 70:2–5
Wayne CE, Wayne RP (1996) Photochemistry. Oxford, UK: Oxford University Press. 98 p

Received August 6, 2014, and approved November 19, 2014.